

## MULTI-SPECTRAL XRF COUNTING: SQUEEZE TWICE AS MUCH INFORMATION FROM YOUR DETECTOR

W.K. Warburton,<sup>1</sup> P. Grudberg,<sup>1</sup> J. Harris,<sup>1</sup> G. Roach<sup>2</sup> and B. Cross<sup>3</sup>

<sup>1</sup>XIA LLC, Newark, CA USA; <sup>2</sup>CSIRO Minerals, Sydney, NSW Australia

<sup>3</sup>Crossroads Scientific, El Granada, CA USA.

### ABSTRACT

Counting small peaks on large backgrounds in XRF applications is a process limited by the statistics of estimating both the counts and the background in the peak region. Improving energy resolution  $\Delta E$  helps by increasing peak/background ratio and providing a more accurate estimate of the background but also reduces counting statistics due to increased pileup losses. Time variant filtering techniques have not been useful because their detector response functions vary with counting rate, precluding the accurate use of standards. Here we present a new time variant approach that takes a small set of shaping filters, applies the longest one to each detector output pulse, and places the result into a spectrum specific to that filter. By not commingling the filters' results, we produce multiple spectra whose detector response functions do not depend upon input count rate and can thus be used with standards-based analyses. Both theoretical and experimental measurements show that this approach allows the filters' information to be fully preserved, so that an optimized multi-spectral spectrometer can achieve the same signal to noise ratio in approximately half the counting time required by an optimized single filter spectrometer.

### INTRODUCTION

A common requirement in XRF measurements is to determine the spectral line intensity  $I_L$  of a weak peak sitting on a large background. Figure 1 indicates the situation schematically. The

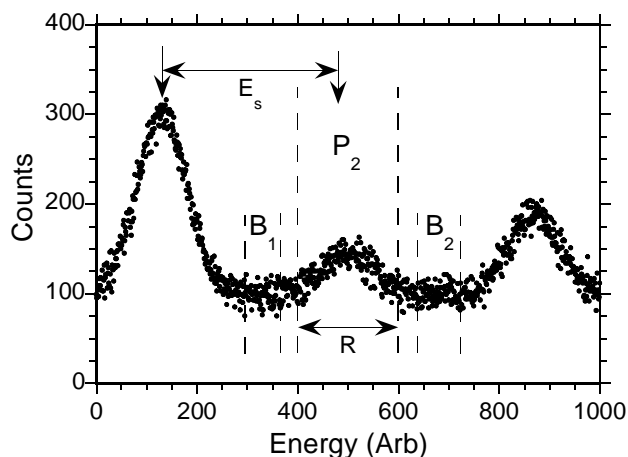


Figure 1: Weak spectral line bounded by neighboring lines.

desired value  $I_L$  is the sum of the counts in a region of interest (ROI)  $P_2$  that includes the peak minus an estimate  $B$  of the background obtained from regions  $B_1$  and  $B_2$ , whose extent is typically limited by neighboring peaks that are separated from the peak of interest by values  $E_s$ . In difficult cases, where  $E_s$  is less than  $R$ , deconvolution methods will be required.  $R$ 's value scales with the spectrometer's energy resolution  $\Delta E$ . For example, for  $R$  to include 95% of the peak area, its value would be  $1.76 \Delta E$ .

In general the statistical accuracy of  $I_L$  can be improved both by collecting more counts, making both the ROI area and background estimates more accurate, and by reducing  $\Delta E$ ,

which both reduces the number of background counts in ROI  $P_2$  and increases the regions  $B_1$  and  $B_2$  over which  $B$  can be measured. Thus, while counting time to a required signal to noise ratio (SNR) can be reduced by increasing output counting rate (OCR) and reducing  $\Delta E$ , these two variables cannot be adjusted independently for a given detector because increasing the OCR requires decreasing the spectrometer's peaking time  $\tau_p$ , which increases  $\Delta E$ . OCR is related to the input count rate ICR by the dead time formula  $OCR = ICR \exp(-\tau_d ICR)$  <sup>(1)</sup>, where  $\tau_d = 2(\tau_p + \tau_g)$  in a digital spectrometer,  $\tau_g$  being a trapezoidal filter's flat top time. Figure 2 shows data from an 80 mm<sup>2</sup> HPGe detector, where counts were collected for 10 sec at the point of maximum

OCR for four  $\tau_p$  values. This particular 60% Fe, 39% Ni and 1% Co sample and was developed to mimic a cobalt stainless steel alloy.

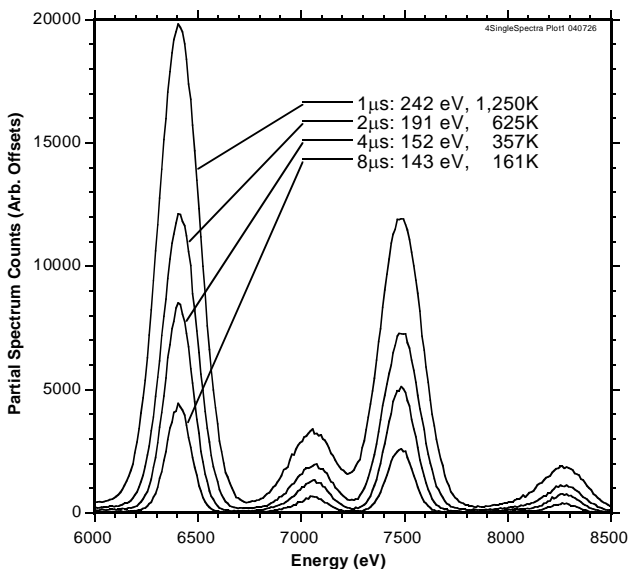


Figure 2: Maximum ICR spectra at 4 peaking times, 10 sec.

### QUALITY FACTOR $Q_f$

The question Figure 2 raises is: “Which spectrum detects the Co best?” We can answer this question by calculating a Quality Factor  $Q_f$ , which is  $1/t_m$ , the time required to collect enough counts to detect a peak of interest to a desired SNR. The system with the largest  $Q_f$  is then the best. Using the terms shown in Figure 1, defining  $K$  as the desired SNR for the peak area minus the background,  $s$  as the line intensity as a fraction of counts in the full spectrum and  $b$  as the background as the fraction of counts in the full spectrum per eV, we derive that:

$$Q_f = \frac{s^2 OCR}{b K^2 R} \left( 1 + \frac{R}{2(E_s - R)} \right)^{-1}, \quad (1)$$

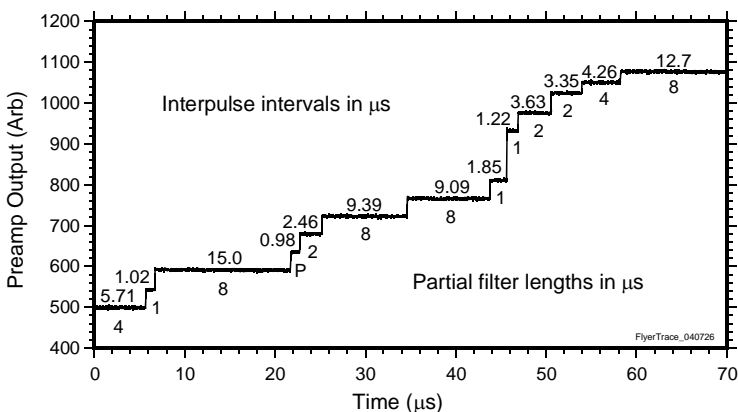
where  $b$  is found by measuring over the background regions  $B_1$  and  $B_2$  whose widths are  $(E_s - R)$ . The maximum of Eqn. 1 versus  $\tau_p$  is then found by using the maximum value  $OCR_{max} = 1/(e \tau_d) = 1/2e(\tau_p + \tau_g)$ , from the throughput equation. The resolution,  $R = 1.76 \Delta E$  can be written as  $R = (R_0 + R_1/\tau_p + R_2\tau_p)^{0.5}$ , where  $R_0$ ,  $R_1$ , and  $R_2$  are constants of the detector. The detector producing the data in Figure 2, for example, had values  $R_0 = 39,558$ ,  $R_1 = 122,121$ , and  $R_2 = 184.4$ . Since the factor  $s^2/(b K^2)$  is a constant, we will compute only the  $\tau_p$  dependent part of  $Q_f$ , namely  $Q_{fp} = Q_f b K^2/s^2$ . Table 1 shows results for  $E_s$  equal to 350 eV, 450 eV, 550 eV, and 650 eV to demonstrate the sensitivity of the results on the widths of regions  $B_1$  and  $B_2$ . As the optimum (bold) results in the four columns show, there is no unique “best” peaking time for all situations. Rather,  $\tau_p$  should be selected depending upon the spectral environment of the peak of interest.

Table 1: Quality factors for five time invariant filters versus  $E_s$ .

$\tau_p$ ( $\mu s$ )	$OCR_{max}$ (kcps)	R (eV)	$Q_{fp}$ for $E_s$ as shown			
			350 eV	450 eV	550eV	650 eV
0.75	175	476	NA	NA	87	156
1.0	141	425	NA	35	123	<b>171</b>
2.0	80	336	18	<b>96</b>	<b>133</b>	155
4.0	43	281	<b>50</b>	83	100	110
8.0	22	234	39	54	62	67

### TIME VARIANT PULSE PROCESSING

The above results are for time invariant filtering. Over the years, various time variant schemes have sought to increase the information extracted from the detector’s signal stream to improve  $\Delta E$  at a given OCR by making better use of the available data. <sup>(2)</sup> Figure 3 demonstrates this approach with some output signal captured from the detector of Figure 2 and Table 1. The pulses in this signal are Poisson distributed, with their intervals indicated in microseconds. Whereas, in time invariant processing, each pulse is analyzed using only 1 peaking time’s data on each side (or rejected as piled up if one of the intervals is too small), in time variant filtering data from full intervals are used to establish the signal levels before and after each pulse. Thus the first pulse may be processed using 5.7  $\mu s$  of leading data and 1.0  $\mu s$  of trailing data; the



**Figure 3:** Preamplifier signal with indicated inter-pulse intervals.

the distribution of inter-pulse intervals varies with ICR and because the relationship between  $\tau_p$  and  $\Delta E$  is non-linear, as per the equation for R used above. Thus “standard” spectra taken at one ICR cannot reliably be used to fit data taken at a different ICR. As a result, time invariant methods have remained the mainstay of modern pulse processing in accurate XRF applications.

### THE MULTI-SPECTRAL (M-S) APPROACH <sup>(3)</sup>

In the M-S approach we retain most of the advantages of time variant filtering while avoiding the variation of  $\Delta E$  with ICR that is its major disadvantage. Our approach is the following. First, we create a small set of M time invariant filters. Second, we process each pulse using the filter that produces the best energy resolution without pileup. Third, we place the result into a spectrum unique to the selected filter. This is the critical step: we do not co-mingle results from filters with different energy resolutions – each spectrum is produced by a single time invariant filter.

In one convenient implementation, we use 16 filters  $F_{ij}$ , each the difference of two running sums  $A_i$  and  $A_j$  separated by a constant gap time  $\tau_g$  and denoted by [i,j]. The length of sum  $A_m$  is  $2^m$  times the length of the shortest sum  $A_1$ , which is set by the worst resolution  $\Delta E$  that can be tolerated in the [1,1] filter. If we set  $A_1$  to  $1\mu s$ , for example, we can process the first pulse in Figure 3 using a [4,1]-filter) and the second pulse using a [1,8]-filter, while the third pulse is piled up because one of its intervals is less than  $1\mu s$ . All results from [4,1]-filtering are placed into a [4,1]-spectrum, all [1,8] results into a [1,8] spectrum, and so forth. Because  $\Delta E$  of an [I,J]-filter and a [J,I] filter are the same, they can share a spectrum, thereby producing 10 unique spectra: [1,1], [1,2], [1,4], [1,8], [2,2], [2,4], [2,8], [4,4], [4,8], and [8,8]. Since each spectrum’s data come from a time invariant filter, its energy resolution will not vary with count rate. The number of counts in each spectra will obviously vary with ICR, with more counts going into the [1,1]-spectrum at high rates and more into the [8,8]-spectrum at low rates, but the shapes of the individual spectra will not vary. Thus a set of standard spectra taken at one ICR can be used to analyze unknowns measured at other ICRs. By separating these filter sums by a flat-top width we can also preserve the benefits of trapezoidal filtering in the M-S approach.

Figure 4 shows a M-S set of the above 10 spectra from the same spectrometer used to produce Figure 2. Because the base [1,1]-filter corresponds to a  $1\mu s$  trapezoidal filter, the total number of counts in all the spectra after 10 seconds of data collection is the same as in Figure 2’s  $1\mu s$  spectrum, 1,250 kcts. While, in Figure 2, they are all in one spectrum with a FWHM of 242 eV, in Figure 4 they are distributed into 10 spectra with FWHM values ranging from 242 to 143 eV. In fact, only 4% of the counts are now in the 242 eV [1,1] spectrum! 12% are in the 218 eV [1,2] spectrum, 12% in the 205 eV [1,4] spectrum, and so on. Surprisingly, the largest number of

second pulse uses  $1.0\mu s$  and  $15.0\mu s$  of data; and so forth. In different flavors of time variant processing the data may be equally or unequally weighted (e.g. with cusp filtering), depending upon their separation from the pulse.

While these methods optimally extract available information, they have not been popular for spectroscopic analysis because their resolution functions vary with ICR. This is both because

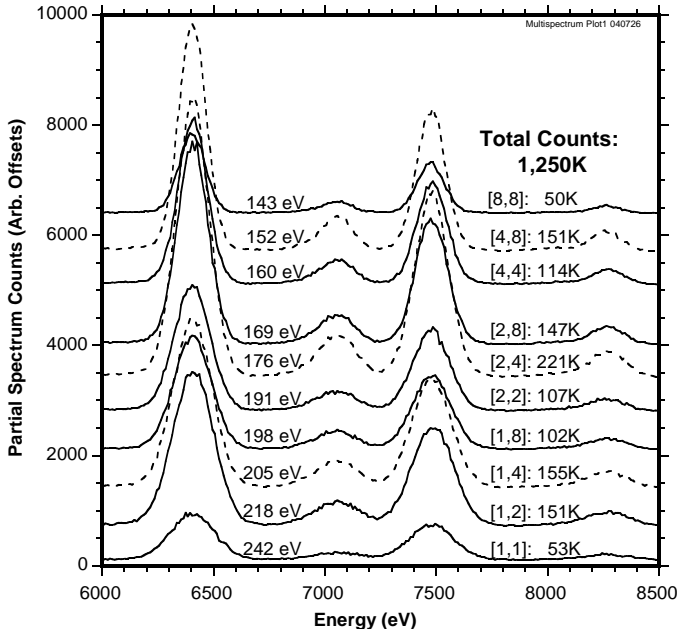


**Figure 4:** Data at 240 kcps ICR sorted into 10 multi-spectra.

10 case's improvement using 16 filters, allowing simplified designs (for example with analog filters) for special purposes or applications where reduced data processing is important.

### M-S QUALITY FACTORS

Extending the single spectrum approach to  $Q_f$  in Eqn. 1 shows that  $Q_f$  in the M-S case is just the sum of the  $Q_f$ 's of the individual  $[i,j]$  spectra and the peaking time dependent term  $Q_{fp}$  becomes:

$$Q_{fp} = \sum_{i,j} \frac{OCR_{i,j}}{R_{i,j}} \left( 1 + \frac{R_{i,j}}{2(E_s - R_{i,j})} \right)^{-1} \quad (2)$$

Eqn. 2 shows explicitly that the additional spectra at higher energy resolutions help in two ways: by decreasing both the resolution  $R_{k,l}$  and the ratio  $R_{k,l}/(E_s - R_{k,l})$ , in the denominator. The first contribution reflects the reduced background component in the ROI integral, the second reflects the increased accuracy with which the background between the peak and its neighbor may be determined. Then, given a value of  $E_s$ , a M-S spectrometer is optimized as follows. First, by extension from the single filter case, an expression is found for the spectrometer's energy resolution as a function of the lengths of the sums in its various filters:

$$R(\tau_i, \tau_j) = [R_0 + R_1 / 2\tau_i + R_1 / 2\tau_j + R_2\tau_i / 2 + R_2\tau_j / 2]^{0.5}. \quad (3)$$

Second, using Poisson statistics, we develop an expression for the filter's output counting rate, realizing that it will process pulses only up to inter-pulse separations that cannot be handled by the next longest set of running sums. Thus we find:

$$OCR(\tau_i, \tau_j) = ICR e^{-2\tau_j} ICR \begin{pmatrix} e^{-\tau_i} ICR & -e^{-\tau_{i+1}} ICR \\ e^{-\tau_j} ICR & -e^{-\tau_{j+1}} ICR \end{pmatrix}. \quad (4)$$

For a particular value of  $E_s$  we can then find an optimum filter in three iterative steps. First, for a pair of values of  $\tau_1$  and ICR, we compute  $Q_p$  as a sum of  $Q_{fp}$  over all 16 filters. Second, we vary ICR to find the maximum  $Q_p$  for that  $\tau_1$  value. Third, we adjust  $\tau_1$  to find the global maximum of  $Q_p$  over both  $\tau_1$  and ICR. Table 2 shows the results of optimizing a 16-filter (i.e. four partial filters) M-S spectrometer to the same four  $E_s$  cases shown in Table 1. Three important features are immediately obvious. First,  $Q_f$  values are improved by factors of nearly 2. Second, the M-S

counts, 18%, is in the 176 eV [2,4] spectrum. The 143 eV [8,8] and 242 eV [1,1] spectra actually have the same number of counts. The average  $\Delta E$  of the set is 184 eV, a substantial improvement over 242 eV. To match this with a single, peaking time filter would require a  $\tau_p$  of about 2.25  $\mu s$ , which would then take over twice as long to collect the same number of counts. We therefore expect the  $Q_f$  of the M-S approach to be about twice that of the best single spectrum system. In general, employing  $M$  starting filters, will then generate  $M' = (M+1)M/2$  unique spectra. Modeling shows that values of  $M$  between 4 and 6 are adequate to achieve most of the benefits of the M-S method ( $M'$  between 10 and 21). Even using just symmetric four filters (i.e. [1,1], [2,2], [3,3] and [4,4]) produces 75% of the  $M' =$

first peaking time is significantly shorter than the single filter optimum because the method has longer peaking times available to achieve better energy resolution when possible. Third, the method achieves substantially higher throughputs than a single filter, because its shorter peaking times can capture pulses that would be piled up in the single filter. These latter two factors explain much of the M-S  $Q_f$  improvement, the remainder coming from the use of separate spectra, so that low resolution data do not "pollute" high resolution spectra, losing information.

**Table 2:** Quality factors using multi-spectral filters, showing gains over single filters.

$E_s$ (eV)	Min $\tau_p$ ( $\mu$ s)	OCR <sub>max</sub> (kcps)	$Q_{fp}$	$Q_{fp}$ Gain (Multi/Single)
350	1.75	74.4	89	1.78
450	0.90	131	178	1.85
550	0.55	187	257	1.93
650	0.40	229	322	1.88

### A FIRST EXPERIMENTAL TEST

Theory and model calculations are all very well, but any new approach needs to be carefully tested experimentally before it is adopted. Here we begin by reporting some initial results with a realistic test case based on a  $Fe_{60}Co_1Ni_{39}$  alloy, which is somewhat difficult because the strong  $Fe-K_\beta$  and  $Ni-K_\alpha$  lines partially overlap the weak  $Co-K_\alpha$  and  $Co-K_\beta$  lines, respectively. We then captured (one at a time) the 10 M-S spectra shown in Fig. 4 and analyzed them using commercial XRF software developed by one of us (BC). In this early work, each M-S spectrum was analyzed independently, the results for each element were summed, and their error counts added in quadrature. Table 3 compares the results of this analysis to those for the 4 single  $\tau_p$  curves shown in Fig. 2. We stress that all spectra were taken for the same 10 second counting time. It may readily be seen that, while there is only modest improvement in the estimates of the majority Fe and Ni peaks, the accuracy for the Co measurement has improved from the best single  $\tau_p$  error of 2.58% to 1.89%, a factor of 0.732, which compares well to the 0.707 expected from a pure factor of 2 improvement in counting efficiency. Since actual improvements in  $Q_f$  are more typically 1.85, however, (per Table 2), and errors scale as  $1/\sqrt{Q_f}$ , we therefore compare  $1/\sqrt{1.85} = 0.735$  to the experimental value 0.732. It thus appears that the method works precisely as expected. This result therefore supports the view that we can expect the Multi-Spectral method to reduce counting times by factors of nearly two to achieve comparable SNR.

**Table 3:** Measured concentrations of Fe, Co and Ni in a  $Fe_{60}Co_1Ni_{39}$  alloy.

$\tau_p$ ( $\mu$ s)	Fe Total (cts)	Fe Error (cts)	Fe Error (%)	Co Total (cts)	Co Error (cts)	Co Error (%)	Ni Total (cts)	Ni Error (cts)	Ni Error (%)
8	65607	512	0.78%	1691	82	<b>4.86%</b>	41331	406	0.98%
4	149607	772	0.52%	3614	120	<b>3.32%</b>	91986	605	0.66%
2	259134	1078	0.42%	4321	111	<b>2.58%</b>	159664	840	0.53%
1	520992	1508	0.29%	5553	156	<b>2.81%</b>	316482	1186	0.37%
M-S	531919	1459	0.27%	11163	211	<b>1.89%</b>	351932	1187	0.34%

### EXTRACTING EMISSION LINE INTENSITIES

In general, the M-S spectra should not be fit independently but simultaneously, since there is physically only a single set of L sample emission line intensities  $\alpha_i$  that will be collected in all spectra simultaneously. Thus, if, in spectrum m, the unit area detector resolution function  $R_{mij}$  describes the intensity in channel j due to a unit strength emission line located in channel i, and there are  $OC_m$  total counts, then the expected counts  $S_{mj}$  in channel j will be given by:

$$S_{mj} = OC_m \sum_{i=1}^L \alpha_i R_{mij}, \quad (5)$$

Here the important points are that the same set of coefficients  $\{\alpha_i, i=1,L\}$  describes the line intensities in all M spectra and that, because the filters are time invariant, the resolution functions  $R_{mij}$  are count rate invariant. To find the  $\alpha$  values by least squares fitting, for example, we would define an error function  $F^M$  and set its partial derivatives with respect to the  $\alpha$ 's to zero:

$$F^M = \sum_{m=1}^{10} \sum_{y_{mj}>0} \left( \frac{y_{mj} - S_{mj}}{\sigma_{mj}} \right)^2 = \sum_{m=1}^{10} \sum_{y_{mj}>0} \left( y_{mj} - OC_m \sum_{i=1}^L \alpha_i R_{mij} \right)^2 \sigma_{mj}^{-2}, \quad (6)$$

giving

$$\frac{\partial F^M}{\partial \alpha_k} = 0 = \sum_{m=1}^{10} \sum_{y_{mj}>0} \left( y_{mj} - OC_m \sum_{i=1}^L \alpha_i R_{mij} \right) \frac{OC_m R_{mkj}}{\sigma_{mj}^2}, \quad (7)$$

where the weighting terms  $\sigma_{mj}$  are Poisson error estimates of the counts  $y_{mj}$ . Rearranging, we get L equations in the L unknown  $\alpha_i$  values

$$\sum_{i=1}^L \alpha_i \left( \sum_{m=1}^{10} OC_m^2 \sum_{y_{mj}>0} (R_{mkj} R_{mij} \sigma_{mj}^{-2}) \right) = \sum_{m=1}^{10} OC_m \sum_{y_{mj}>0} (R_{mkj} y_{mj} \sigma_{mj}^{-2}) \quad (8)$$

and, assuming there are enough counts per channel to allow approximating  $\sigma_{mj}^2$  by  $y_{mj}$ , find:

$$\sum_{i=1}^L \alpha_i \left( \sum_{m=1}^{10} OC_m^2 \sum_{y_{mj}>0} (R_{mkj} R_{mij} y_{mj}^{-1}) \right) = \sum_{m=1}^{10} OC_m \sum_{y_{mj}>0} R_{mkj} \quad (9)$$

This exercise shows that the major change in adapting an existing algorithm for processing a single spectrum (no sums over m) to processing M-S spectra is that sums over the single spectrum are summed again over the M-S spectra in setting up the linear equations to solve for the  $\alpha_i$  values representing the unknown emission line strengths. Adapting to M-S spectral processing should therefore be a relatively straightforward operation in most cases.

## CONCLUSIONS

We have introduced a time variant, Multi-Spectral signal processing method for use in XRF spectrometers. In M-S filtering, a small set of time invariant filters sort results into a set of output spectra whose resolution functions do not vary with input counting rate, each signal pulse being processed by the optimum member of the set. We have shown that the method works in a simple system and also shown that, when detecting small peaks on large backgrounds, it essentially halves the counting time required to achieve a specified signal to noise ratio. Further, adapting existing data processing algorithms to the new method should be readily achievable.

## REFERENCES

- 1: G.F. Knoll, *Radiation Detection and Measurement*, 2<sup>nd</sup> Ed., (J. Wiley, 1989), Chapter 4, Sect. VII, pp. 120-128.
- 2: A good review may be found in R.B. Mott & J.J. Friel, "Improving Detection Limits with Digital Pulse Processing", in *X-ray Spectrometry in Electron Beam Instruments*, Eds. DB Williams, JI Goldstein & DE Newbury (Plenum, 1995).
- 3: W.K. Warburton et al., US PCT Patent Application PCT/US 11/142,819, June 2005. Published as US-2006-0015290-A1 on January 19, 2006.